HHS Public Access

Author manuscript

Inorg Chem. Author manuscript; available in PMC 2019 September 17.

Published in final edited form as:

Inorg Chem. 2018 September 17; 57(18): 11696–11703. doi:10.1021/acs.inorgchem.8b01830.

Supramolecular Pt(II) and Ru(II) Trigonal Prismatic Cages Constructed with a Tris(pyridyl)borane Donor

Ji Yeon Ryu[†], **Ji Min Lee**[†], **Nguyen Van Nghia**[‡], **Kang Mun Lee**[§], **Sunwoo Lee**[†], **Min Hyung Lee**[‡,*], **Peter J. Stang**[‖,*], and **Junseong Lee**[†,*]

[†]Department of Chemistry, Chonnam National University, Gwangju 61186, Republic of Korea

[‡]Department of Chemistry and EHSRC, University of Ulsan, Ulsan 44610, Republic of Korea

[§]Department of Chemistry, Institute for Molecular Science and Fusion Technology, Kangwon National University, Chuncheon, Gangwon 24341, Republic of Korea

[‖]Department of Chemistry, University of Utah, 315 South 1400 East, Room 2020, Salt Lake City, Utah 84112, United States

Abstract

We report a novel example of supramolecular cages containing a Lewis acidic trigonal boron center. Self-assembly of the tris(pyridyl)borane donor **1** with diruthenium (**2**) or platinum (**3**), as an electron acceptor, furnished boron-containing trigonal prismatic supramolecular cages **5** and **6**, which were characterized by ^{1}H NMR and electrospray ionization time-of-flight mass spectroscopy and X-ray crystallography. The molecular structure of cage **5** was confirmed as a trigonal prismatic cage with an inner dimension of about 400 Å^{3}. The fluoride binding properties of borane ligand **1** and Pt cage **6** were studied. UV/Vis absorption titration studies demonstrated that the boron center of cage **6** undergoes strong binding interaction with the fluoride ion, with an estimated binding constant of 1.3×10^{10} M^{-2} in acetone based on the 1:2 binding isotherm. The binding was also confirmed by ^{1}H NMR titration. Photoluminescence titration studies showed that cage **6** emitted borane-centered fluorescence ($\tau = 2.21$ ns), which was gradually quenched upon addition of fluoride. When excess fluoride was added to a solution of **6**, however, dissociation of the pyridyl ligand from the Pt(II) center was observed.

Graphical Abstract

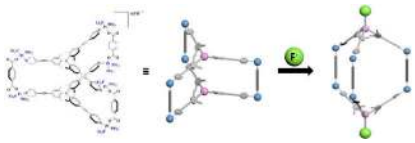

[*]**Corresponding Authors:** lmh74@ulsan.ac.kr, Stang@utah.edu, leespy@chonnam.ac.kr.

Supporting Information

The Supporting Information is available free of charge on the ACS Publications website at DOI: 0.1021/.

Experimental procedures; analytical data for boron lig- and **1** and cages **5** and **6** with ^{1}H, ^{13}C NMR and ESI-TOF-MS spectra; X-ray crystallographic data for **1** and **5** in cif format.

The authors declare no competing financial interests.

The self-assembly of a C_3-symmetric tris(pyridyl)borane ligand and diruthenium or platinum electron acceptors led to the formation of trigonal prismatic supramolecular cages. The boron centers in the ligand and the platinum cage readily complexed fluoride anions, exhibiting turn-off fluorescence responses upon the addition of fluoride anions.

INTRODUCTION

The successful synthesis of supramolecular cages via coordination-driven self-assembly[1–17] has contributed not only to the design and synthesis of various two-dimensional (2-D) and three-dimensional (3-D) nanoscale architectures,[18] but also to various applications, including specific organic or organometallic reactions,[19] optical sensors, and anticancer agents.[20–21] Recent investigations in supramolecular chemistry have focused on the interactions of these cages with specific anions[22], cations, carboxylic acids,[23] or amino acids due to the increasing interest in biological applications.[24] For example, we and Yang's group reported halide or amino acid sensing of supramolecules by means of metal-halide or metal-amino acid interactions.[25] However, there are limited examples of supramolecules that possess hetero-atom functional groups in the electron donor ligands.[26–27]

As a novel functional moiety, we have been interested in tri-coordinate organoboron compounds as they can serve as Lewis acidic sites in supramolecules. Triarylborane compounds and transition metal complexes[28–29] decorated with triarylboryl groups have been widely investigated in many applications such as catalysis[30–32], frustrated Lewis pairs[33–36], organic light-emitting diodes (OLEDs),[37–45] and anion sensors[42, 46–49] during recent decades. In anion-sensing applications, the geometry of the boron center is altered from trigonal planar to tetrahedral by complexation with Lewis bases such as fluoride and cyanide anions.[50] This structural transformation often results in changes in the fluorescence or absorption, allowing for the detection of anions (Scheme 1).[51] In spite of extensive studies in these areas, triarylborane has not been incorporated into supramolecular cage systems that may provide interesting photophysical and structural features. To date, only supramolecular assemblies containing four-coordinate boron moieties such as 4,4-difluoro-4-bora-3a,4a-diaza-s-indacene (BODIPY)[52–54] and those with dative boron-nitrogen bonds[55–57] have been reported.

To achieve unique self-assembly of Lewis acidic boron-containing supramolecular cages, we designed a tris(pyridyl)borane donor ligand and the corresponding trigonal prismatic cages. It was envisioned that the introduction of the pyridyl donor units bearing a triarylborane moiety into the metal acceptor units should lead to the formation of novel Lewis acidic supramolecules possessing a discrete trigonal prismatic structural framework and cavity. Two kinds of metal acceptors were selected, i.e., diruthenium and *cis*-type platinum complexes, for self-assembly (Scheme 2). The diruthenium complex can act as a molecular clip to bind two parallel pyridine groups. Because the *cis*-type platinum complex has two binding sites with a connectivity of 90°, the dibenzoate ligand was used as a pillar to bind two platinum centers and to support the trigonal prismatic framework. In this study, we report the construction of hexanuclear ruthenium and platinum cages containing Lewis

acidic trigonal boron centers, and investigate their structural, photophysical, and fluoride binding properties.

EXPERIMENTAL DETAILS

General Considerations

Diethylamine was distilled from sodium hydroxide, and tetrahydrofuran (THF) was distilled from K(s)/benzophenone. Deuterated solvents were purchased from EURISO-TOP. All other reagents were purchased (Aldrich or Acros) and used without further purification. Tris(4-bromo-2,6-methylphenyl)borane[58] and the diruthenium complex **2**[59] were synthesized according to the reported procedures. The melting points (mp) were determined on an Electrothermal melting point apparatus. NMR spectra were recorded on a Bruker AVANCE III HD 400 instrument (400 MHz) at ambient temperature. The ^{1}H and ^{13}C NMR chemical shifts are reported relative to the residual peaks of $CDCl_3$ (^{1}H; 7.26 ppm, ^{13}C; 77.0 ppm), CD_3OD (3.30 ppm), and $(CD_3)_2CO$ (2.05 ppm), whereas the ^{31}P NMR resonances are referenced to an external unlocked sample of 85% H_3PO_4 (δ 0.0). High-resolution mass spectroscopy–electrospray ionization time-of-flight (HRMS–ESI-TOF) spectroscopy was performed on the SYNAPT G2 instrument at the Ochang Branch of the Korean Basic Science Institute. ESI-TQ-MS spectra were recorded on a Finnigan TSQ Quantum Ultra EMR spectrometer, using electrospray ionization, at the Seoul Branch of the Korean Basic Science Institute. Elemental analysis (C, H, and N) was performed with an EA1110-FISONS (CE) instrument. Diffusion-ordered spectroscopy (^{1}H ^{2}D-DOSY) measurements were carried out with a Varian Unity-Inova 600 MHz instrument. Samples with concentrations of 5–10 mM were used for the diffusion NMR experiments to reduce the viscosity changes and intermolecular interactions. The hydrodynamic radii were calculated according to the spherical approximation using the Einstein-Stokes equation.

Synthesis of Tris(2,6-dimethyl-4-(2-(trimethylsilyl)ethynyl)phenyl)borane (1a)

A solution of tris(4-bromo-2,6-methylphenyl)borane (1.00 g, 1.77 mmol), $PdCl_2(PPh_3)_2$ (18.7 mg, 0.026 mmol), and CuI (5.07 mg, 0.026 mmol) in dried diethylamine (15 mL) and THF (5.0 mL) was added dropwise to a solution of ethynyltrimethylsilane (1.01 mL, 7.10 mmol) in diethylamine (3.0 mL) at room temperature under N_2 atmosphere. After stirring for 1 h, the mixture was heated to reflux for 12 h. After cooling to room temperature, distilled water was added and the mixture was extracted with diethyl ether. The extract was dried over anhydrous $MgSO_4$, filtered, and concentrated under reduced pressure. The crude product was purified by column chromatography on silica gel (hexane, R_f = 0.2) to give compound **1a** in 60% yield (0.65 g) as a white powder. IR (KBr-disk, cm^{-1}): 2959(m), 2153(m), 1594(m), 1289(m), 841(s). ^{1}H NMR ($CDCl_3$, 400 MHz): δ 0.24 (s, 27H, $Si(CH_3)_3$), 1.94 (s, 18H, 2,6-Me_2Ph), 7.06 (s, 6H, Ph). ^{13}C NMR ($CDCl_3$, 100 MHz): δ 22.66, 30.88, 94.87, 105.24, 124.13, 131.10, 140.48, 146.89. mp = 253 °C. Anal. calcd. for $C_{39}H_{51}BSi_3$•1/3Et_2NH: C, 75.78; H, 8.62; N, 0.73. Found: C, 75.29; H, 8.71; N, 0.66.

Synthesis of Tris(4-ethynyl-2,6-dimethylphenyl)borane (1b)

1a (200 mg, 0.325 mmol) and KOH (219 mg, 3.90 mmol) were stirred in a mixed solvent of MeOH (15 mL) and THF (8.0 mL) for 2 h at room temperature under N_2 atmosphere. After

removal of the solvent, water was added and the mixture was extracted with diethyl ether. The organic layer was separated and dried over anhydrous $MgSO_4$. Filtration followed by concentration of the filtrate under reduced pressure afforded a crude mixture. The resulting mixture was washed with hexane and filtered, which gave **1b** in 85% yield as a white powder (110 mg). IR (KBr-disk, cm^{-1}): 2923(m), 2100(w), 1593(m), 1409(m), 836(s). ^1H NMR ($CDCl_3$, 400 MHz): δ 1.97 (s, 18H, 2,6-*Me*$_2$Ph), 3.08 (s, 3H, ethynyl), 7.08 (s, 6H, Ph). ^{13}C NMR ($CDCl_3$, 100MHz): δ 22.72, 77.66, 83.79, 123.26, 131.31, 140.55, 147.02. mp = >300 °C. HRMS (ESI-TOF): 399.2284 (calcd. for $C_{30}H_{28}B$ $[M-H]^+$ 399.2279). Anal. calcd. for $C_{30}H_{27}B•0.6C_4H_8O•0.3CH_2Cl_2$: C, 84.01; H, 7.02. Found: C, 84.09; H, 6.99.

Synthesis of Tris(2,6-dimethyl-4-(2-(pyridin-4-yl)ethynyl)phenyl)borane (1)

1b (200 mg, 0.50 mmol), 4-iodopyridine (360 mg, 1.75 mmol), $PdCl_2(PPh_3)_2$ (17.5 mg, 0.025 mmol), and CuI (9.52 mg, 0.05 mmol) were dissolved in piperidine (10 mL) at room temperature and the mixture was stirred for 24 h under N_2 atmosphere. The resulting mixture was filtered through Celite and the filtrate was dried under reduced pressure. The crude product was subjected to column chromatography on silica gel (EtOAc/hexane, 7:3), giving **1** in 30% yield (94 mg) as an ivory powder. X-ray quality crystals were grown by the slow diffusion of hexane into the ethyl acetate solution. IR (KBr-disk, cm^{-1}): 2212(m), 1596(s), 1411(m), 1204(m). ^1H NMR ($CDCl_3$, 400 MHz): δ 2.05 (s, 18H, 2,6-*Me*$_2$Ph), 7.18 (s, 6H, Ph), 7.41 (d, 6H, pyr), 8.60 (d, 6H, pyr). ^{13}C NMR ($CDCl_3$, 100MHz): δ 22.81, 87.31, 94.38, 123.28, 123.31, 125.59, 125.63, 131.10, 131.69, 131.84, 140.78, 147.46, 149.32, 149.45. ^{11}B NMR ($CDCl_3$, 128 MHz): δ 75.6. mp = 284 °C. HRMS (ESI-TOF): 630.3079 (calcd. for $C_{45}H_{37}BN_3$ $[M-H]^+$ 630.3075). Anal. calcd. for $C_{45}H_{36}BN_3•CH_2Cl_2$: C, 77.32; H, 5.36; N, 5.88. Found: C, 77.73; H, 5.32; N, 6.20.

Preparation of Trigonal Prism 5

Ligand **1** (3.0 mg, 4.76 μmol), diruthenium precursor **2** (5.2 mg, 7.14 μmol), and silver triflate (3.6 mg, 14.3 μmol) were dissolved in 0.4 mL of MeOH-d_4. The mixture was stirred for 2 h in the dark at room temperature. The resulting mixture was filtered through a membrane filter. Slow diffusion of diethyl ether into the solution at room temperature produced deep green crystals of **5** that were suitable for X-ray crystallographic analysis (yield = 18.6 mg, 95%). IR (KBr-disk, cm^{-1}): 1535 (s), 1274 (m), 1157 (w), 1030 (m). ^1H NMR (MeOH-d_4, 400 MHz): δ 1.33 (dd, 36H, - CH(C*H*$_3$)$_2$), 1.80 (s, 18H, 2,6-*Me*$_2$Ph), 2.04 (s, 18H, 2,6-*Me*$_2$Ph), 2.10 (s, 18H, *p*-cymene), 2.82 (sep, 6H, -C*H*(CH$_3$)$_2$), 5.63 (d, 12H, *p*-cymene), 5.84 (d, 12H, *p*-cymene), 7.09 (s, 6H, Ph), 7.24 (m, 18H, Ph+nq), 7.47 (dd, 12H, pyr), 8.41 (dd, 12H, pyr). ESI-TQ-MS: 1915.87 (calcd. for [**5**-2OTf]$^{2+}$ 1915.80) 1227.91 (calcd. for [**5**-3OTf]$^{3+}$ 1227.51). Anal. calcd. for $C_{186}H_{168}B_2F_{18}N_6O_{30}Ru_6S_6•3CH_2Cl_2$: C, 51.77; H, 4.00; N, 1.92. Found: C, 51.68; H, 4.03; N, 1.86.

Preparation of Trigonal Prism 6

Ligand **1** (3.0 mg, 4.76 μmol), disodium terephthalate (2.0 mg, 7.14 μmol), *cis*-$(PEt_3)_2PtCl_2$ (7.2 mg, 14.3 μmol), and silver tri-flate (6.1 mg, 23.8 μmol) were dissolved in acetone/water (4:1, v/v). The mixture was stirred for 12 h at 50 °C in the dark. The resulting mixture was filtered through a membrane filter and the solvent was evaporated. The residue was

redissolved in acetone and filtered. The filtrate was poured into excess diethyl ether to form a precipitate, which was collected by centrifugation to give a beige powder in 95% yield (11.8 mg). IR (KBr-disk, cm^{-1}): 2969 (w), 2211 (w), 1610 (m), 1416 (w), 1261 (s), 1032 (s), 638 (m). ^{1}H NMR (acetone-d_6, 400 MHz): δ 1.32 (m, 108H, PCH_2CH_3), 1.97 (m, 72H, PCH_2CH_3), 2.06 (s, 36H, 2,6-Me_2Ph), 7.26 (d, 12H, Ph), 7.74 (m, 24H, pyr+terephthalate), 8.98 (br, 12H, pyr). ^{31}P{^{1}H} NMR (acetone-d_6): δ –1.13 (d, $^2J_{P-P}$ = 21.6 Hz, ^{195}Pt satellites, $^1J_{Pt-P}$ = 3425 Hz), 4.37 (d, $^2J_{P-P}$ = 21.6 Hz, ^{195} Pt satellites, $^1J_{Pt-P}$ = 3222 Hz). ESI-TQ-MS (m/z): 1594.67 (calcd. for $[M-3OTf]^{3+}$ 1594.79). Anal. Calcd. for $C_{198}H_{264}B_2F_{36}N_6O_{48}P_{12}Pt_6S_{12}$•1.5$C_3H_6O$•2$H_2O$: C, 38.9; H, 4.47; N, 1.34. Found: C, 38.7; H, 4.66; N, 1.24.

Photophysical and Fluoride Binding Measurements

UV/Vis absorption and PL spectra were recorded on a Varian Cary 100 and a HORIBA FluoroMax-4P spectrophotometer, respectively, at room temperature. The solution samples of ligand **1** and complex **6** were prepared in acetone using a 1 cm quartz cuvette. Emission lifetimes were measured on a FS5 spectrophotometer (Edinburgh Instruments) equipped with an EPL-375 picosecond pulsed diode laser at 298 K. The quantum yields (PLQYs) of the solutions were measured on an absolute PL quantum yield spectrophotometer (Quantaurus-QY C11347–11, Hamamatsu Photonics) equipped with a 3.3 inch integrating sphere. Fluoride titration experiments were carried out with the addition of incremental amounts of fluorides (Bu_4NF). The detailed conditions are given in the figure captions. The absorbance data were fitted to a 1:1 binding isotherm for ligand **1**[60–62] and a 1:2 for **6**[63] to evaluate the binding constant (K).

X-Ray Structure Determination

Reflection data for **1** and **5** were collected on a Bruker APEX-II CCD-based diffractometer with graphite-monochromated MoKα radiation (λ = 0.7107 Å). The hemisphere of the reflection data was collected as ω scan frames at 0.5°/frame using an exposure time of 5 s/frame. The cell parameters were determined and refined by using the APEX2 program.[64] The data were corrected for Lorentz and polarization effects. An empirical absorption correction was applied using the SADABS program. The structures of the compounds were solved by direct methods and refined by full matrix least-squares methods using the SHELXTL program package with anisotropic thermal parameters for all non-hydrogen atoms.[65] The data are summarized in Table S1. CCDC 1578330–1578331 contains the supplementary crystallographic data for this study. These data can be obtained free of charge from The Cambridge Crystallographic Data Centre via www.ccdc.cam.ac.uk/data_request/cif. The crystals of **1** and **5** provided very weak diffraction due to the large amount of disordered solvents and anions. Geometrical restraints, i.e. DFIX, SADI, SIMU, and AFIX 66 on part of the hexagonal aromatic rings, were used in the refinements.

RESULTS AND DISCUSSION

As a new electron donor system containing a Lewis acidic triarylboron moiety, tris(pyridyl)borane ligand **1** was designed and prepared (Scheme 3). To endow the boron center with steric protection, the *ortho*-dimethyl-substituted aryl-4-pyridyl group was

introduced to the boron center. Starting from tris(4-bromo-2,6-methylphenyl)borane,[58] Sonogashira coupling with ethynyltrimethylsilane followed by desilylation produced ethynyl-substituted triarylborane (**1b**). **1b** was further subjected to Sonogashira coupling with 4-iodopyridine, leading to the tris(pyridyl)borane lig- and **1**. Ligand **1** was characterized by means of various methods, including ^{1}H and ^{11}B NMR spectroscopy and mass spectrometry. Additionally, X-ray crystallography confirmed the molecular structure of compound **1** (Figure 1). The central boron atom adopts a trigonal planar geometry (Σ(C-B-C) = 359.9°), as consistent with the broad ^{11}B signal at 76 ppm. Three Ar groups form a propeller-like conformation due to steric repulsion between the six *ortho*-methyl groups around the boron atom. Compound **1** has a *C*3 principal axis, but possesses only pseudo-*D*3 point group symmetry due to the disorder of the pyridine groups, which likely arises from the rotational flexibility of the pyridine. As a result, the pyridine rings are tilted by as much as 45–49° out of the plane of the Ar groups.

Construction of Trigonal Prismatic Supramolecules 5 and 6

Trigonal prismatic cages **5** and **6** were prepared by the self-assembly of the tris(pyridyl)borane connector **1** and diruthenium acceptor **2** or platinum acceptor **3** (Scheme 4). The reaction of borane connector **1**, diruthenium complex **2**, and AgOTf in a molar ratio of 2:3:6 afforded the trigonal prismatic cage **5**. Whereas, in the synthesis of Pt-B cage, dibnezoate complex **4** was additionally used as a pillar. From the reaction of borane connector **1**, platinum complex **3**, dibenzoate **4**, and AgOTf in a molar ratio of 2:3:3:6, desired cage **6** was easily obtained. The formation of cages **5** and **6** was established by ^{1}H NMR spectroscopy and electron ionization time-of-flight mass spectrometry (ESI-TOF-MS). The ^{1}H NMR spectra confirmed the existence of a single product in the reaction mixture and showed a diagnostic shift of the pyridyl protons (δ = 8.41 and 7.47 ppm for **5**, 8.94 and 7.74 ppm for **6**) when compared to those of the borane donor ligand (δ = 8.63 and 7.53 ppm) (Figure 2).

The formation of trigonal prismatic cages **5** and **6** was also confirmed by the ESI-TOF-MS spectra, as shown in Figure 3. The ESI-TOF-MS peaks of **5** and **6** are attributable to the loss of triflate ions $[M - 2OTf]^{2+}$ (m/z = 1918.87 (**5**)) and $[M - 3OTf]^{3+}$ (m/z = 1227.91 (**5**) and 1594.67(**6**)), where M represents the intact assemblies.

Additionally, X-ray crystallography unequivocally confirmed the molecular structure of complex **5** (Figure 4). Despite the low data quality for the crystal due to its weak diffraction, the molecular structure and connectivity of the cation component could be clearly observed. The cation of complex **5** was confirmed to be a hexanuclear ruthenium trigonal prismatic supramolecular cage consisting of six half-sandwich Ru units, and two borane ligands with an inside dimension of about 400 Å^3 (ca. 7.5 ~ 7.8 Å in height and ca. 23 Å in width), as estimated using the six Ru vertices. Notably, the propeller-like conformation of the two triarylborane units prevented π-stacking interaction between these units. Moreover, the long distance (ca. 7.8 Å) between the two boron centers excludes the possibility of π-π interaction. Consequently, complex **5** did not show strong M/P double-rossette helicity, which has been observed in other trigonal prismatic cages, and provided ΔΛ propeller isomerism around the boron centers.

Photophysical and Fluoride Binding Properties of Ligand 1 and Cage 6

The borane ligand **1** and cage **6** were used in the fluoride ion binding study. Cage **5** was found to be unstable in the presence of fluoride ions. To investigate the binding interaction of the boron centers in ligand **1** and cage **6**, ^{1}H NMR titration experiments with the fluoride anion were first carried out in acetone-d_6 (Figures 5 and S17-S18). The results show that the intensity of the H_α and H_β peaks of the pyridyl group in **1** and **6** decreased upon gradual addition of fluoride anions. The peaks completely disappeared after the addition of over 1.0 equiv of fluoride for **1** (Figure 5b) and 2.0 equiv for **6** (Figure 5d) and shifted to the up-field region. Simultaneously, the diagnostic C_{Ar}–H resonances at δ ca. 7.2 ppm for the 2,6-$Me_2C_6H_2$ rings in the borane moieties of both **1** and **6** underwent splitting into two broad singlets in the up-field region after fluoride addition. Further the ^{11}B signal of cage **6** in the presence of 2.0 equiv of fluoride appeared at δ ca. 6 ppm, which is typical for fluoroborate species (Figure S24). These results indicate that all of the trigonal boron centers in **1** and **6** bind with fluoride ions, forming tetracoordinated fluoroborates. However, when more than 2.0 equiv of fluoride ions was added to the solution of cage **6**, the ^{1}H signals corresponding to [**1**–F]$^{-}$ began to appear, indicating slow dissociation of the pyridyl ligand from the Pt(II) center.

Based on these results, we examined the photophysical and fluoride binding properties of **1** and **6** in detail using UV/Vis absorption and photoluminescence (PL) spectroscopy. The titration experiments were carried out in acetone (Figure 6). Ligand **1** features a broad low-energy absorption band centered at 357 nm, which was gradually quenched upon addition of incremental amounts of fluoride (Figure 6a).[58] The complete quenching of the low-energy absorption bands after 1.0 equiv fluoride addition is similar to that observed in the ^{1}H NMR titrations above. This finding further indicates that the low-energy absorption in ligand **1** is mainly assignable to the triarylborane-centered, $\pi \rightarrow p_\pi(B)$ charge transfer (CT) transition.[66–68] The resulting fluoride binding constant (K) was estimated to be ca. 2.0×10^6 M^{-1} in acetone from the 1:1 binding isotherm (Figure S21).[60–62] Strong fluorescence (PLQY = 0.39, τ = 2.62 ns) centered at 410 nm was also observed in the PL spectrum of **1**. The broad spectral profile further indicates the CT excited state of ligand **1**. Upon the addition of fluoride, efficient fluorescence quenching was observed as a result of fluoride binding to the boron center of **1** (Figure 6b).

Cage **6** exhibited a strong low-energy absorption at 365 nm that was slightly red-shifted compared to the band of ligand **1**. The absorption bands are gradually quenched upon addition of fluoride anions (Figure 6c). Although substantial absorption from the resulting fluoroborate species remained after the titration, the quenching of the absorption is associated with fluoride binding to the boron centers in cage **6**. This finding also suggests that the red-shift of the absorption in cage **6** relative to that of **1** could be due to the lowering of the LUMO level by coordination of the pyridyl lone pair electrons to the Pt center.[69–70] The observation of clear isosbestic points around 388 nm implies exclusion of reactions other than fluoride binding. The binding stoichiometry determined from the Job's plot indicates a 1:2 binding ratio between cage **6** and fluoride (Figure S20), which is also consistent with the ^{1}H NMR titration results presented above. The fluoride binding constant of cage **6** was estimated to be approximately 1.31×10^{10} $[M]^{-2}$ from the 1:2 binding

isotherm.[71] The changes in the PL spectra of cage **6** upon fluoride addition were also investigated (Figure 6d). Cage **6** exhibited a broad, strong emission (PLQY = 0.28) centered at 415 nm, which was slightly red-shifted, but similar to that of ligand **1**, indicating a tris(pyridyl)borane-centered emission. The emission lifetime (τ) measured from the transient PL decay was 2.21 ns, confirming the proposed fluorescence origin of the emission. The intensity of the emission band of **6** was gradually quenched upon addition of fluoride. This result is in parallel with fluoride binding to the boron centers in **6**. While fluorescence quenching occurred stably up to the addition of 4 equiv fluoride, the addition of excess fluoride slowly resulted in decomposition of the cage structure due to dissociation of the Pt–N(pyd) bonds by the fluoride anion.

CONCLUSIONS

Two trigonal prismatic cages **5** and **6**, composed of tris(pyridyl)borane donor **1** and diruthenium acceptor **2** or platinum acceptor **3**, were prepared. Cages **5** and **6** were characterized by various spectroscopic methods, and the molecular structures of donor **1** and cage **5** were confirmed by X-ray crystallography. The trigonal prismatic cage **5** possessed inner dimension of about 400 $Å^3$ with base-free trigonal boron centers. The photophysical and fluoride binding properties of donor ligand **1** and its corresponding cage **6** were investigated by the ^1H NMR and UV/Vis absorption and PL titrations. The Lewis acidic boron centers in cage **6** readily complexed fluoride anions, with an estimated binding constant of 1.3×10^{10} M^{-2} in acetone from the 1:2 binding isotherms. Both the donor ligand **1** and cage **6** similarly exhibited a turn-off fluorescence response upon fluoride binding. The results in this study may provide a new avenue for the construction and applications of functional supramolecules.

Supplementary Material

Refer to Web version on PubMed Central for supplementary material.

ACKNOWLEDGMENT

J.L. acknowledges financial support from the Basic Science Research Program (2016R1D1A1B03930507) and BRL Program (2015R1A4A1041036) through the National Research Foundation of Korea (NRF), funded by the Ministry of Science, ICT & Future Planning and Education. P.J.S. thanks the NIH (R01-CA215157) for financial support. M.H.L thanks the NRF (2017R1A2B4002468) for financial support.

REFERENCES

(1). Brown CJ; Toste FD; Bergman RG; Raymond KN Supramolecular Catalysis in Metal-Ligand Cluster Hosts. Chem. Rev 2015, 115, 3012–3035. [PubMed: 25898212]

(2). Saalfrank RW; Maid H; Scheurer A Supramolecular Coordination Chemistry: The Synergistic Effect of Serendipity and Rational Design. Angew. Chem. Int. Ed 2008, 47, 8794–8824.

(3). Oliveri CG; Ulmann PA; Wiester MJ; Mirkin CA Heteroligated Supramolecular Coordination Complexes Formed via the Halide-Induced Ligand Rearrangement Reaction. Acc. Chem. Res 2008, 41, 1618–1629. [PubMed: 18642933]

(4). Caulder DL; Bruckner C; Powers RE; Konig S; Parac TN; Leary JA; Raymond KN Coordination number incommensurate cluster formation, part 21 - Design, formation and properties of tetrahedral M4L4 and M4L6 supramolecular clusters. J. Am. Chem. Soc 2001, 123, 8923–8938. [PubMed: 11552799]

(5). Fujita D; Ueda Y; Sato S; Mizuno N; Kumasaka T; Fujita M Self-assembly of tetravalent Goldberg polyhedra from 144 small components. Nature 2016, 540, 563–566.

(6). Sun W-Y; Kusukawa T; Fujita M Electrochemically Driven Clathration/Declathration of Ferrocene and Its Derivatives by a Nanometer-Sized Coordination Cage. J. Am. Chem. Soc 2002, 124, 11570–11571. [PubMed: 12296702]

(7). Harris K; Fujita D; Fujita M Giant hollow MnL2n spherical complexes: structure, functionalisation and applications. Chem. Commun 2013, 49, 6703–6712.

(8). Gianneschi NC; Masar MS; Mirkin CA Development of a Coordination Chemistry-Based Approach for Functional Supramolecular Structures. Acc. Chem. Res 2005, 38, 825–837. [PubMed: 16285706]

(9). Saha ML; Schmittel M From 3-Fold Completive Self-Sorting of a Nine-Component Library to a Seven-Component Scalene Quadrilateral. J. Am. Chem. Soc 2013, 135, 17743–17746. [PubMed: 24224927]

(10). De S; Mahata K; Schmittel M Metal-coordination-driven dynamic heteroleptic architectures. Chem. Soc. Rev 2010, 39, 1555–1575. [PubMed: 20419210]

(11). Smulders MMJ; Riddell IA; Browne C; Nitschke JR Building on architectural principles for three-dimensional metallosupramolecular construction. Chem. Soc. Rev 2013, 42, 1728–1754. [PubMed: 23032789]

(12). McConnell AJ; Wood CS; Neelakandan PP; Nitschke JR Stimuli-Responsive Metal–Ligand Assemblies. Chem. Rev 2015, 115, 7729–7793. [PubMed: 25880789]

(13). Cook TR; Stang PJ Recent Developments in the Preparation and Chemistry of Metallacycles and Metallacages via Coordination. Chem. Rev 2015, 115, 7001–7045. [PubMed: 25813093]

(14). Cook TR; Zheng YR; Stang PJ Metal-Organic Frameworks and Self-Assembled Supramolecular Coordination Complexes: Comparing and Contrasting the Design, Synthesis, and Functionality of Metal-Organic Materials. Chem. Rev 2013, 113, 734–777. [PubMed: 23121121]

(15). Schmitt F; Freudenreich J; Barry NPE; Juillerat-Jeanneret L; Süss-Fink G; Therrien B Organometallic Cages as Vehicles for Intracellular Release of Photosensitizers. J. Am. Chem. Soc 2012, 134, 754–757. [PubMed: 22185627]

(16). Severin K Supramolecular chemistry with organometallic half-sandwich complexes. Chem. Commun 2006, 3859–3867.

(17). Christinat N; Scopelliti R; Severin K Multicomponent Assembly of Boronic Acid Based Macrocycles and Cages. Angew. Chem. Int. Ed 2008, 47, 1848–1852.

(18). Lehn J Supramolecular chemistry. Science 1993, 260, 1762–1763. [PubMed: 8511582]

(19). Brown CJ; Toste FD; Bergman RG; Raymond KN Supramolecular Catalysis in Metal–Ligand Cluster Hosts. Chem. Rev 2015, 115, 3012–3035. [PubMed: 25898212]

(20). Vajpayee V; Yang YJ; Kang SC; Kim H; Kim IS; Wang M; Stang PJ; Chi KW Hexanuclear self-assembled arene-ruthenium nano-prismatic cages: potential anticancer agents. Chem. Commun 2011, 47, 5184–5186.

(21). Pitto-Barry A; Zava O; Dyson PJ; Deschenaux R; Therrien B Enhancement of Cytotoxicity by Combining Pyrenyl-Dendrimers and Arene Ruthenium Metallacages. Inorg. Chem 2012, 51, 7119–7124. [PubMed: 22716166]

(22). Li Z-Y; Zhang Y; Zhang C-W; Chen L-J; Wang C; Tan H; Yu Y; Li X; Yang H-B Cross-Linked Supramolecular Polymer Gels Constructed from Discrete Multi-pillar[5]arene Metallacycles and Their Multiple Stimuli-Responsive Behavior. J. Am. Chem. Soc 2014, 136, 8577–8589. [PubMed: 24571308]

(23). Vajpayee V; Song YH; Lee MH; Kim H; Wang M; Stang PJ; Chi KW Self-Assembled Arene-Ruthenium-Based Rectangles for the Selective Sensing of Multi-Carboxylate Anions. Chem. Eur. J 2011, 17, 7837–7844. [PubMed: 21611989]

(24). Neelakandan PP; Jimenez A; Nitschke JR Fluorophore incorporation allows nanomolar guest sensing and white-light emission in M4L6 cage complexes. Chem. Sci 2014, 5, 908–915.

(25). Zhang M; Saha ML; Wang M; Zhou Z; Song B; Lu C; Yan X; Li X; Huang F; Yin S; Stang PJ Multicomponent Platinum(II) Cages with Tunable Emission and Amino Acid Sensing. J. Am. Chem. Soc 2017, 139, 5067–5074. [PubMed: 28332834]

(26). Han M; Engelhard DM; Clever GH Self-assembled coordination cages based on banana-shaped ligands. Chem. Soc. Rev 2014, 43, 1848–1860. [PubMed: 24504200]

(27). Schmidt A; Hollering M; Han J; Casini A; Kuhn FE Self-assembly of highly luminescent heteronuclear coordination cages. Dalton Trans. 2016, 45, 12297–12300. [PubMed: 27436541]

(28). Rajendra Kumar G; Thilagar P Tuning the Phosphorescence and Solid State Luminescence of Triarylborane-Functionalized Acetylacetonato Platinum Complexes. Inorg. Chem 2016, 55, 12220–12229. [PubMed: 27934401]

(29). Sakuda E; Funahashi A; Kitamura N Synthesis and Spectroscopic Properties of Platinum(II) Terpyridine Complexes Having an Arylborane Charge Transfer Unit. Inorg. Chem 2006, 45, 10670–10677. [PubMed: 17173422]

(30). Erker G Tris(pentafluorophenyl)borane: a special boron Lewis acid for special reactions. Dalton Trans. 2005, 1883–1890. [PubMed: 15909033]

(31). Piers WE, The Chemistry of Perfluoroaryl Boranes In Advances in Organometallic Chemistry, Academic Press: 2004; Vol. 52, pp 1–76.

(32). Chen EY-X; Marks TJ Cocatalysts for Metal-Catalyzed Olefin Polymerization: Activators, Activation Processes, and Structure–Activity Relationships. Chem. Rev 2000, 100, 1391–1434. [PubMed: 11749269]

(33). W. SD; Gerhard E Frustrated Lewis Pairs: Metal-free Hydrogen Activation and More. Angew. Chem. Int. Ed 2010, 49, 46–76.

(34). Stephan DW Activation of dihydrogen by non-metal systems. Chem. Commun 2010, 46, 8526–8533.

(35). Stephan DW "Frustrated Lewis pairs": a concept for new reactivity and catalysis. Organic & Biomolecular Chemistry 2008, 6, 1535–1539. [PubMed: 18421382]

(36). Welch GC; Juan RRS; Masuda JD; Stephan DW Reversible, Metal-Free Hydrogen Activation. Science 2006, 314, 1124–1126. [PubMed: 17110572]

(37). Lee YH; Park S; Oh J; Shin JW; Jung J; Yoo S; Lee MH Rigidity-Induced Delayed Fluorescence by Ortho Donor-Appended Triarylboron Compounds: Record-High Efficiency in Pure Blue Fluorescent Organic Light-Emitting Diodes. ACS Appl. Mater. Interfaces 2017, 9, 24035–24042. [PubMed: 28653832]

(38). Hatakeyama T; Shiren K; Nakajima K; Nomura S; Nakatsuka S; Kinoshita K; Ni J; Ono Y; Ikuta T Ultrapure Blue Thermally Activated Delayed Fluorescence Molecules: Efficient HOMO–LUMO Separation by the Multiple Resonance Effect. Adv. Mater 2016, 28, 2777–2781. [PubMed: 26865384]

(39). Katsuaki S; Shosei K; Katsuyuki S; Tatsuya F; Atsushi W; Yasujiro M; Chihaya A; Hironori K Triarylboron-Based Fluorescent Organic Light-Emitting Diodes with External Quantum Efficiencies Exceeding 20 %. Angew. Chem. Int. Ed 2015, 54, 15231–15235.

(40). Yang X; Zhou G; Wong W-Y Functionalization of phosphorescent emitters and their host materials by main-group elements for phosphorescent organic light-emitting devices. Chem. Soc. Rev 2015, 44, 8484–8575. [PubMed: 26245654]

(41). Yang X; Sun N; Dang J; Huang Z; Yao C; Xu X; Ho C-L; Zhou G; Ma D; Zhao X; Wong W-Y Versatile phosphorescent color tuning of highly efficient borylated iridium(iii) cyclometalates by manipulating the electron-accepting capacity of the dimesitylboron group. J. Mater. Chem. C 2013, 1, 3317–3326.

(42). Hudson ZM; Wang S Impact of Donor–Acceptor Geometry and Metal Chelation on Photophysical Properties and Applications of Triarylboranes. Acc. Chem. Res 2009, 42, 1584–1596. [PubMed: 19558183]

(43). Zhou G; Ho CL; Wong WY; Wang Q; Ma D; Wang L; Lin Z; Marder Todd B; Beeby A Manipulating Charge-Transfer Character with Electron-Withdrawing Main-Group Moieties for the Color Tuning of Iridium Electrophosphors. Adv. Funct. Mater 2008, 18, 499–511.

(44). Tanaka D; Takeda T; Chiba T; Watanabe S; Kido J Novel Electron-transport Material Containing Boron Atom with a High Triplet Excited Energy Level. Chem. Lett 2007, 36, 262–263.

(45). Entwistle CD; Marder TB Applications of Three-Coordinate Organoboron Compounds and Polymers in Optoelectronics. Chem. Mater 2004, 16, 4574–4585.

(46). Zhao H; Leamer LA; Gabbai FP Anion capture and sensing with cationic boranes: on the synergy of Coulombic effects and onium ion-centred Lewis acidity. Dalton Trans. 2013, 42, 8164–8178. [PubMed: 23599021]

(47). Wade CR; Broomsgrove AEJ; Aldridge S; Gabbaï FP Fluoride Ion Complexation and Sensing Using Organoboron Compounds. Chem. Rev 2010, 110, 3958–3984. [PubMed: 20540560]

(48). Jäkle F Advances in the Synthesis of Organoborane Polymers for Optical, Electronic, and Sensory Applications. Chem. Rev 2010, 110, 3985–4022. [PubMed: 20536123]

(49). Hudnall TW; Chiu C-W; Gabbaï FP Fluoride Ion Recognition by Chelating and Cationic Boranes. Acc. Chem. Res 2009, 42, 388–397. [PubMed: 19140747]

(50). Yamaguchi S; Akiyama S; Tamao K Colorimetric fluoride ion sensing by boron-containing pi-electron systems. J. Am. Chem. Soc 2001, 123, 11372–11375. [PubMed: 11707112]

(51). Chiu C-W; Kim Y; Gabbaï FP Lewis Acidity Enhancement of Triarylboranes via Peripheral Decoration with Cationic Groups. J. Am. Chem. Soc 2009, 131, 60–61. [PubMed: 19093849]

(52). Dsouza RN; Pischel U; Nau WM Fluorescent Dyes and Their Supramolecular Host/Guest Complexes with Macrocycles in Aqueous Solution. Chem. Rev 2011, 111, 7941–7980. [PubMed: 21981343]

(53). Xu L; Wang Y-X; Yang H-B Recent advances in the construction of fluorescent metallocycles and metallocages via coordination-driven self-assembly. Dalton Trans. 2015, 44, 867–890. [PubMed: 25429665]

(54). Gupta G; Das A; Ghate NB; Kim T; Ryu JY; Lee J; Mandal N; Lee CY Novel BODIPY-based Ru(ii) and Ir(iii) metalla-rectangles: cellular localization of compounds and their antiproliferative activities. Chem. Commun 2016, 52, 4274–4277.

(55). Icli B; Sheepwash E; Riis-Johannessen T; Schenk K; Filinchuk Y; Scopelliti R; Severin K Dative boron-nitrogen bonds in structural supramolecular chemistry: multicomponent assembly of prismatic organic cages. Chem. Sci 2011, 2, 1719–1721.

(56). Sheepwash E; Luisier N; Krause MR; Noe S; Kubik S; Severin K Supramolecular polymers based on dative boron-nitrogen bonds. Chem. Commun 2012, 48, 7808–7810.

(57). Sheepwash E; Krampl V; Scopelliti R; Sereda O; Neels A; Severin K Molecular Networks Based on Dative Boron-Nitrogen Bonds. Angew. Chem. Int. Ed 2011, 50, 3034–3037.

(58). Lee KM; Kim Y; Do Y; Lee J; Lee MH Synthesis and Fluoride Binding Properties of Tris-pyridinium Borane. Bull. Korean Chem. Soc 2013, 34, 1990–1994.

(59). Yan H; Suss-Fink G; Neels A; Stoeckli-Evans H Mono-, di- and tetra-nuclear p-cymeneruthenium complexes containing oxalato ligands. Dalton Trans. 1997, 4345–4350.

(60). Kim Y; Gabbaï FP Cationic Boranes for the Complexation of Fluoride Ions in Water below the 4 ppm Maximum Contaminant Level. J. Am. Chem. Soc 2009, 131, 3363–3369. [PubMed: 19256571]

(61). Solé S; Gabbaï FP A bidentate borane as colorimetric fluoride ion sensor. Chem. Commun 2004, 1284–1285.

(62). Sharma S; Kim H; Lee YH; Kim T; Lee YS; Lee MH Heteroleptic Cyclometalated Iridium(III) Complexes Supported by Triarylborylpicolinate Ligand: Ratiometric Turn-On Phosphorescence Response upon Fluoride Binding. Inorg. Chem 2014, 53, 8672–8680. [PubMed: 25090619]

(63). Liu XY; Bai DR; Wang S Charge-Transfer Emission in Nonplanar Three-Coordinate Organoboron Compounds for Fluorescent Sensing of Fluoride. Angew. Chem. Int. Ed 2006, 45, 5475–5478.

(64). Bruker AXS (2014). APEX2. Version 2014.11–0. Madison, Wisconsin, USA.

(65). Sheldrick G Crystal structure refinement with SHELXL. Acta Cryst. C 2015, 71, 3–8.

(66). Huh Jung Oh; Kim Hyungjun; Lee Kang Mun; Lee Yoon Sup; Do Youngkyu; Lee MH o-Carborane-assisted Lewis acidity enhancement of triarylboranes. Chem. Commun 2010, 46, 1138.

(67). Youngmin Kim; Gabbaï FP Cationic Boranes for the Complexation of Fluoride Ions in Water below the 4 ppm Maximum Contaminant Level. J. Am. Chem. Soc 2009, 131, 3363–3369. [PubMed: 19256571]

(68). Hudnall Todd W.; Gabbaï F. o. P. Ammonium Boranes for the Selective Complexation of Cyanide or Fluoride Ions in Water. J. Am. Chem. Soc 2007, 129, 11978–11986. [PubMed: 17845043]

(69). Sun Y; Wang S Conjugated Triarylboryl Donor–Acceptor Systems Supported by 2,2 ′-Bipyridine: Metal Chelation Impact on Intraligand Charger Transfer Emission, Electron Accepting Ability, and "Turn-on" Fluoride Sensing. Inorg. Chem 2009, 48, 3755–3767. [PubMed: 19256481]

(70). Sun Y; Ross N; Zhao S-B; Huszarik K; Jia W-L; Wang R-Y; Macartney D; Wang S Enhancing Electron Accepting Ability of Triarylboron via π-Conjugation with 2,2'-Bipy and Metal Chelation: 5,5'-Bis(BMes2)-2,2'-bipy and Its Metal Complexes. J. Am. Chem. Soc 2007, 129, 7510–7511. [PubMed: 17530762]

(71). Liu Xiang Yang; Bai Dong Ren; Wang S Charge-Transfer Emission in Nonplanar Three-Coordinate Organoboron Compounds for Fluorescent Sensing of Fluoride. Angew. Chem. Int. Ed 2006, 45, 5475–5479.

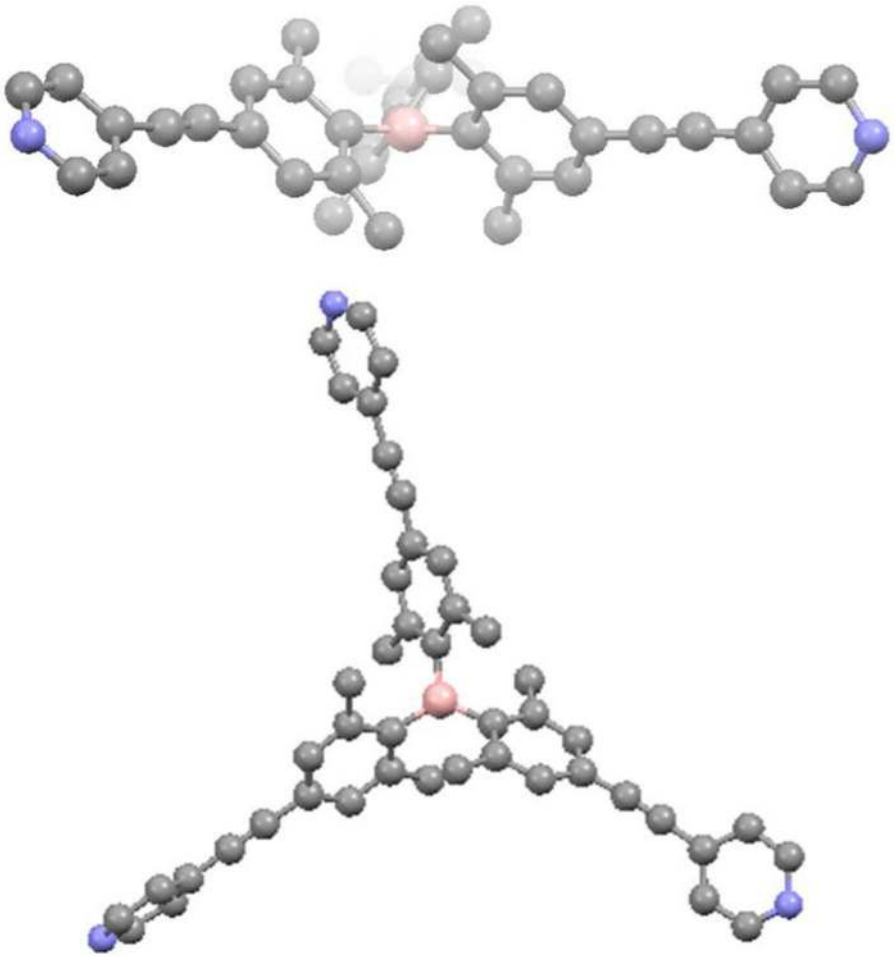

Figure 1.

X-ray structure of tris(pyridyl)borane ligand **1**: (top) side-view and (bottom) top-view. Color code: pink = B; sky-blue = N. Hydrogen atoms are omitted for clarity.

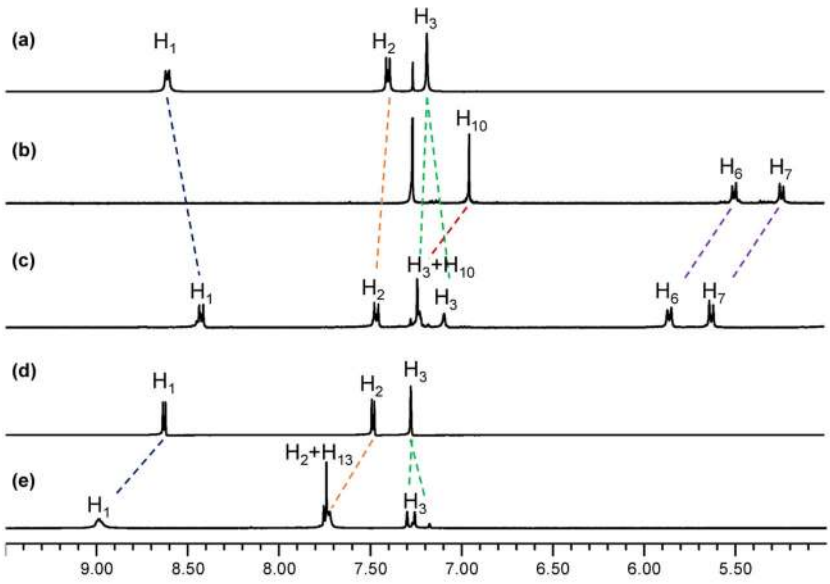

Figure 2.

Comparison of the partial ^{1}H NMR spectra. (a) tritopic pyridylborane ligand **1** in $CDCl_3$, (b) diruthenium complex **2** in $CDCl_3$, (c) trigonal prismatic cage **5** in MeOD. (d) tritopic pyridylborane ligand **1**, and (e) trigonal prismatic cage **6** in aceton-d_6.

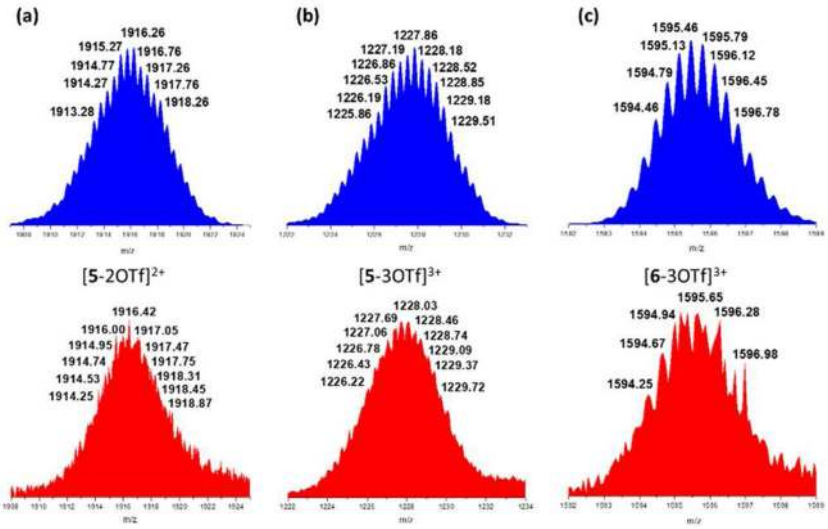

Figure 3.

Comparison of calculated (blue) and experimental (red) ESI-TOF-MS spectra of supramolecular boron complexes (a) [**5**-2OTf]$^{2+}$, (b) [**5**-3OTf]$^{3+}$, and (c) [**6**-3OTf]$^{3+}$.

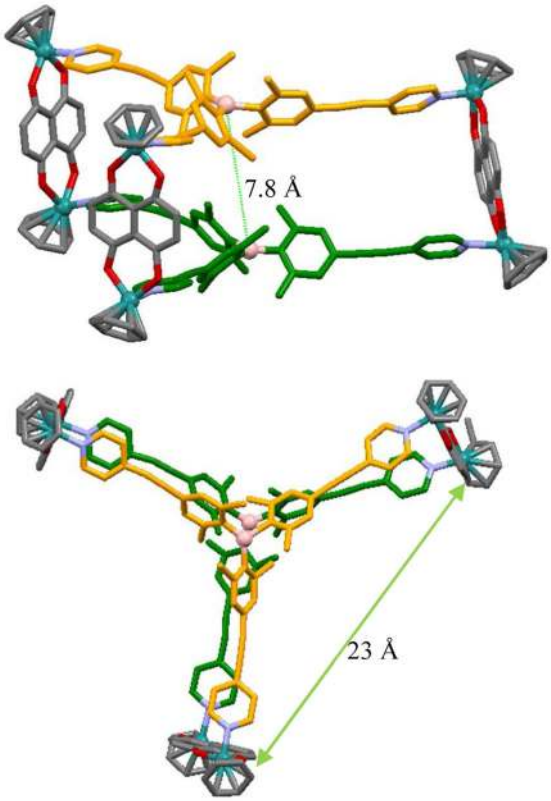

Figure 4.

Wireframe representation of the X-ray structure of trigonal-prismatic cage **5**: side-view (top) and top-view (bottom). Color code: green = Ru; pink = B; red = O; sky-blue = N. Hydrogen atoms and counteranions are omitted for clarity.

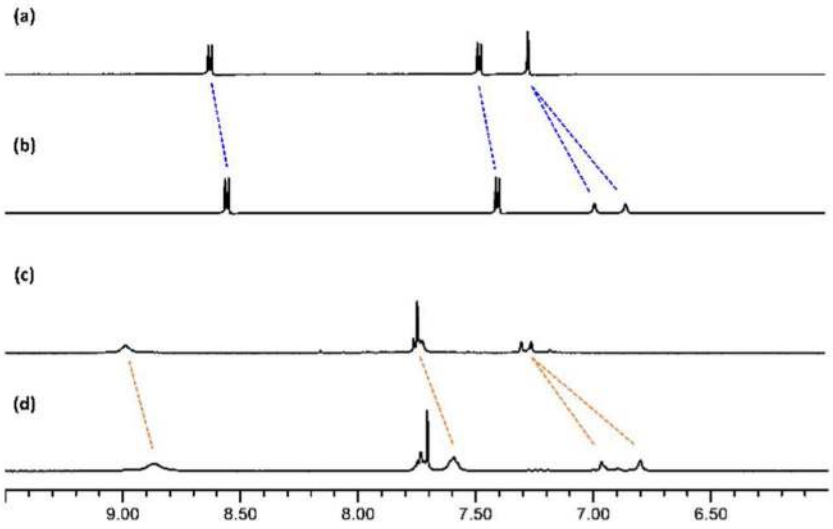

Figure 5.

Comparison of the partial ^{1}H NMR spectra of (a) tritopic pyridylborane ligand **1**, (b) after addition of 1. 0 equiv of TBAF to ligand, (c) trigonal prismatic cage **6**, and (d) after addition of 2.0 equiv of TBAF to cage **6**.

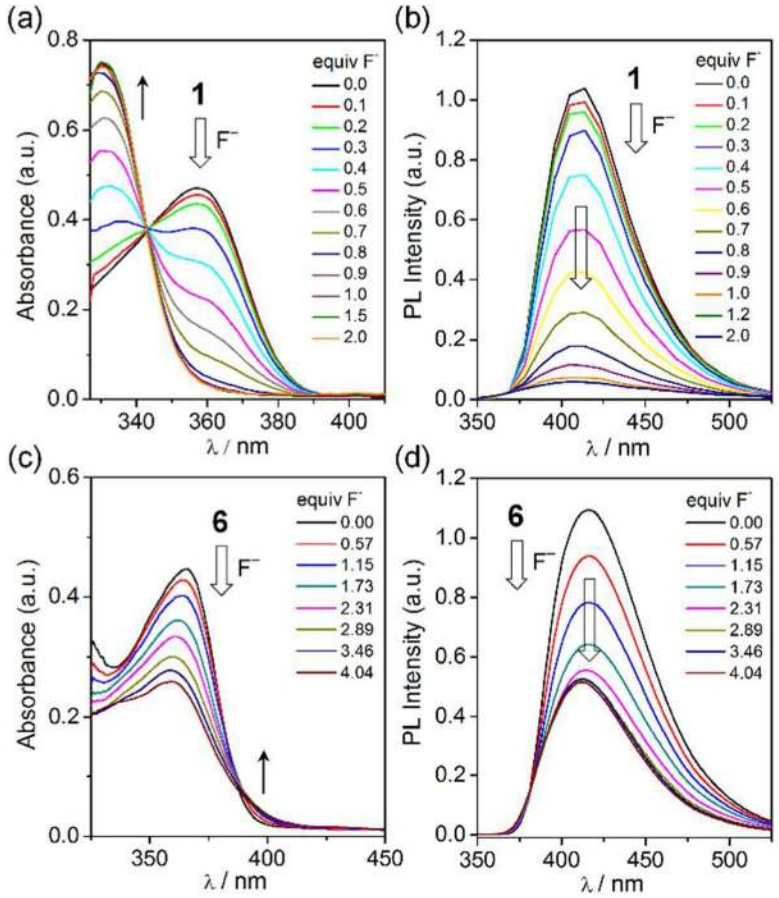

Figure 6.

Changes in the UV/Vis absorption (left) and PL (right) spectra of ligand **1** (top; 1.00×10^{-5} M; 0–2.0 equiv Bu_4NF) and cage **6** (bottom; 3.32×10^{-6} M; 0–4.04 equiv Bu_4NF) in acetone upon addition of fluoride anions. High-energy absorption region of acetone (cut-off) is not shown.

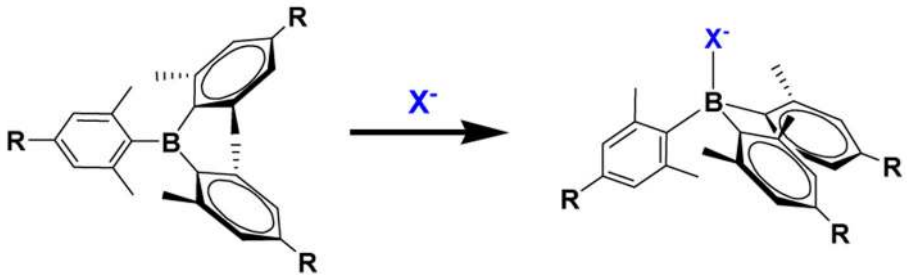

Scheme 1.

Geometrical change of trigonal boron center upon anion (X^-) binding.

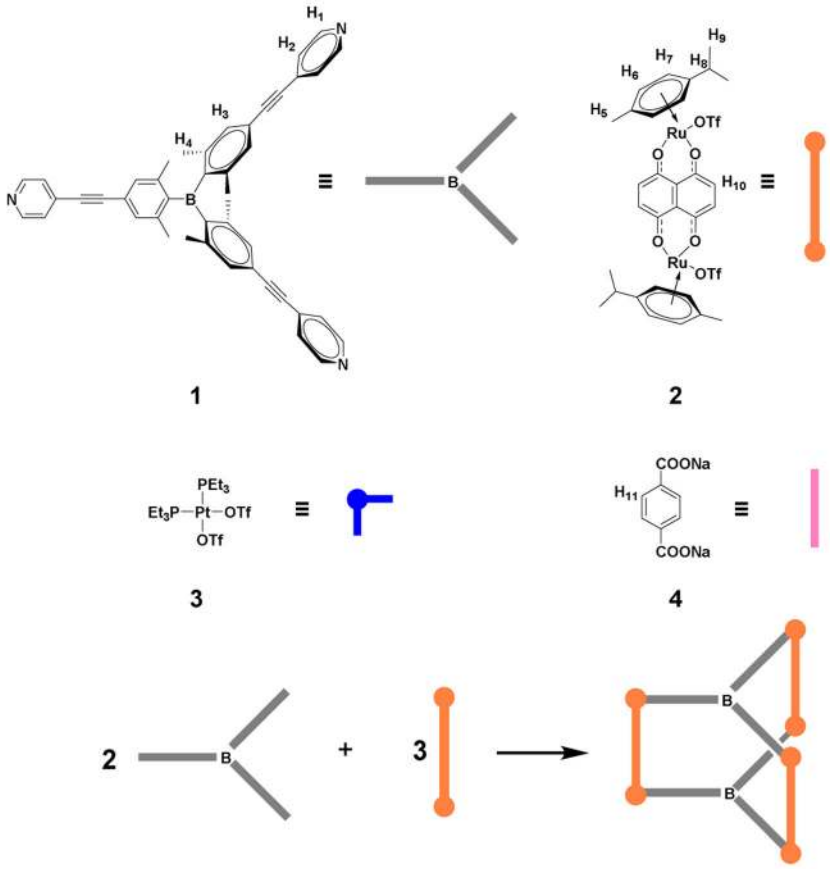

Scheme 2.

Electron donor and acceptor molecules and the coordination-driven self-assembly of trigonal prismatic cages.

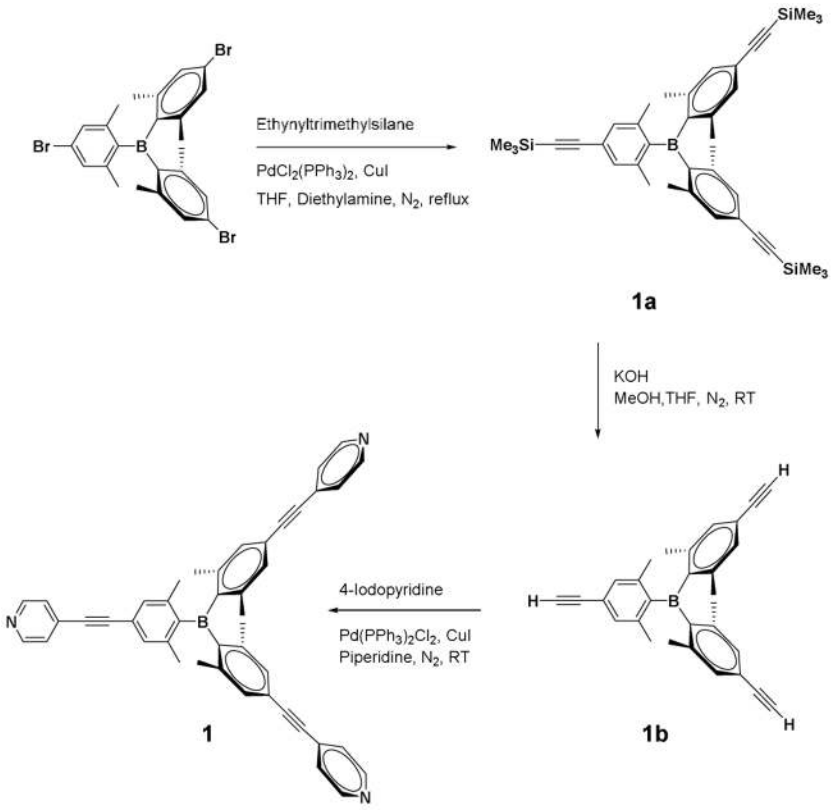

Scheme 3.
Synthesis of tritopic pyridylborane ligand **1**.

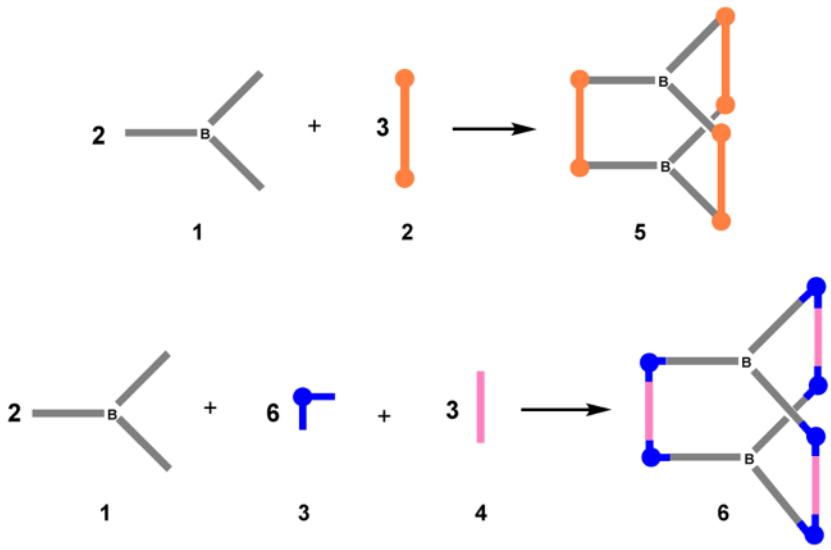

Scheme 4.

Coordination-driven self-assembly of trigonal prismatic supramolecules **5** and **6**.